

The effect of processing conditions on the phase, microstructure and dielectric properties of SrCa₄Nb₄TiO₁₇ and Ca₅Nb₄TiO₁₇ microwave ceramics

A. MANAN^{1,2*}, I.M. REANEY²

¹ Department of Physics, University of Science and Technology Bannu, Postcode 28100, Pakistan

² Department of Materials Science and Engineering Materials, Sir Robert Hadfield Building, University of Sheffield, S1 3JD UK

The effect of processing conditions on the phase, microstructure and dielectric properties of SrCa₄Nb₄TiO₁₇ and Ca₅Nb₄TiO₁₇ microwave ceramics was investigated. The ceramics processed via solid state mixed-oxide route were characterized using XRD, Raman spectroscopy and SEM for phase, molecular vibrational modes and microstructural analysis respectively. Dielectric properties at low and microwave frequencies were measured using LCR meter and a vector network analyzer. The XRD results revealed the formation of a single phase for each ceramics. The microstructure was comprised of elongated and plate-like grains. The optimum microwave dielectric properties *i.e.* temperature coefficient of resonant frequency (τ_f) ~ -78 ppm/K, electric permittivity (ϵ_r) ~ 47.2 and quality factor multiplied by the resonant frequency ($Q_u f_o$) ~ 11954 GHz, were achieved for SrCa₄Nb₄TiO₁₇, sintered at 1475 °C for 4 h. For Ca₅Nb₄TiO₁₇, sintered at 1450 °C for 4 h, the respective properties were: $\tau_f \sim -137$ ppm/K, $\epsilon_r \sim 42$ and $Q_u f_o \sim 14800$ GHz respectively.

Keywords: SEM, perovskites, processing, dielectric resonators

© Wrocław University of Technology.

1. Introduction

Recent technological developments in the wireless telecommunication systems utilizing microwave dielectric ceramics as resonators, filters and other components, have increased the interest in designing and engineering of new materials for better performance and miniaturization of the microwave components. Ideal materials for commercial applications as dielectric resonators (DRs) are required to have $\epsilon_r > 24$, $\tau_f \sim 0$ ppm/K, and a high $Q_u f_o$ (~ 30000 GHz) values at microwave frequencies. For certain applications *e.g.* antennas, the requirements for low values of τ_f and high $Q_u f_o$ are flexible to some extent *e.g.* $\tau_f \pm 10$ ppm/K and $Q_u f_o > 10,000$ GHz are acceptable; however, ϵ_r must be high enough to miniaturize the device for incorporation into a handset. Additionally, as given by Eq. 1, the use of a high ϵ_r material is important for reducing the size and weight and hence

manufacturing and operational cost of the electronic equipment [1].

$$\lambda_d \propto 1/(\epsilon_r)^{1/2} \quad (1)$$

where λ_d is the wavelength in a dielectric given by $\lambda_d = \lambda_o/(\epsilon_r)^{1/2}$.

Several materials have their commercial applications as DRs in handsets and base stations but there is still a continuous search for materials with ultra low losses, $\tau_f \sim 0$ ppm/K and high electric permittivity [2–5].

A number of dielectric materials belonging to $A_n B_n O_{3n+2}$ ($n = 5$) series with good microwave dielectric properties have been investigated for practical applications at microwave frequencies [6–11]. Recently, the authors [12] investigated the microwave dielectric properties of the compounds in the Sr_{5-x}Ca_xNb₄TiO₁₇ ($x = 0-5$) series. The compounds with $x = 4$ and 5, *i.e.* SrCa₄Nb₄TiO₁₇ and Ca₅Nb₄TiO₁₇, sintered at 1500 °C for 2 h at heating/cooling rates of 5 °C/min, were reported to exhibit the optimum properties with $\epsilon_r \sim 42.2$

*E-mail: Abdul_manan_sher@yahoo.co.uk

and 37.6, $Q_{uf_o} \sim 1166$ GHz and 3087 GHz and $\tau_f \sim -86.0$ ppm/K and -132.5 ppm/K respectively. The Q_{uf_o} values were too low for microwave applications. However, in another study, $\text{Ca}_5\text{Nb}_4\text{TiO}_{17}$ was reported to have $\epsilon_r \sim 44.9$, $\tau_f \sim -112.9$ ppm/K with good $Q_{uf_o} \sim 17600$ GHz [13], which are much better than the ones we reported for $\text{Ca}_5\text{Nb}_4\text{TiO}_{17}$ in our previous study [12]. The difference among the properties obtained for $\text{Ca}_5\text{Nb}_4\text{TiO}_{17}$ ceramics by Joseph *et al.* [13] and by the authors might be attributed to the different processing conditions employed and the formation of a secondary phase in the authors' previous study [12]. It is also reported that such factors as secondary phase formation [14, 15], grain and particle size [15, 16], processing conditions, like milling time [17], calcination temperature, calcination and sintering durations [18–21], impurities in raw materials, and contamination from milling media [22, 23] have a great influence on the microwave dielectric properties particularly the quality factor of the materials.

Therefore, the present study was aimed on the processing of $\text{SrCa}_4\text{Nb}_4\text{TiO}_{17}$ and $\text{Ca}_5\text{Nb}_4\text{TiO}_{17}$ under processing conditions different from the ones in the previous study in an attempt to improve the microwave dielectric properties of the ceramics.

2. Materials and method

Stoichiometric amounts of SrCO_3 (Aldrich, 99+ %), CaCO_3 (Aldrich, 99+ %), Nb_2O_5 (Aldrich, 99.95 %), TiO_2 (Aldrich, Anatase, 99+ %) were weighed to prepare $\text{SrCa}_4\text{Nb}_4\text{TiO}_{17}$ and $\text{Ca}_5\text{Nb}_4\text{TiO}_{17}$ batches. The carbonates were heated at ~ 180 °C, while the oxides were heated at ~ 900 °C over a night prior to the weighing to remove the moisture and to assure the correct initial stoichiometry. The mixed batches were ball milled for 24 h in disposable polyethylene mill-jars using Y-toughened ZrO_2 balls as grinding media and isopropanol as a lubricant. The resulting slurries were dried over a night at ~ 95 °C. Thermal (TG/DTA) analysis was performed from room temperature to 1200 °C at 10 °C/min for the as-mixed milled powders to determine the weight loss and phase transformation temperatures. The milled powders were calcined for 6 h at 1300 °C and 1400 °C at a heat-

ing/cooling rate of 5 °C/min for $\text{SrCa}_4\text{Nb}_4\text{TiO}_{17}$ and $\text{Ca}_5\text{Nb}_4\text{TiO}_{17}$ batches respectively. The calcined powders were finely ground in a pestle and a mortar for ~ 45 min and then pressed into 2–4 mm high and 10 mm in diameter pellets at ~ 100 MPa. The pellets were sintered at 1425–1500 °C for 4 h at a heating/cooling rate of 5 °C/min. The phase analysis of calcined and sintered crushed pellets was carried out using a Philips X-ray diffractometer, operating at 30 kV and 40 mA at 1°/min from $2\theta = 10 - 70^\circ$ with a step size of 0.02°. A STOE PSD X-ray diffractometer with CuK_α radiation ($\lambda = 1.540598$ Å) was used for the measurement of lattice parameters. The optimally sintered pellets were thoroughly polished and then etched at a temperature lower by 10 % than the corresponding sintering temperatures. Afterward, the microstructural characterization was performed using a scanning electron microscope (JEOL JSM-6400, Tokyo, Japan) operating at 20 kV. The bulk apparent densities of the sintered pellets were measured using Archimedes method. The theoretical densities of the compounds were calculated using Eq. 2:

$$\rho_{th} = ZM/VA_g \quad (2)$$

where Z is the formula unit, M is the molecular weight, V is the volume of the unit cell and A_g is the Avogadro number (6.022×10^{23} atoms/mole).

The faces of the sintered pellets were coated with gold paste and heated to 800 °C for 2 h at heating/cooling rates of 10 °C/min. The dielectric properties were measured in the range of 1 kHz – 1 MHz using HP 4384A LCR meter. Microwave dielectric properties were measured using a R3767CH Agilent network analyzer. The cylindrical pellets were placed on a low loss quartz single crystal at the centre of the Au coated brass cavity proposed by Krupka [24]. τ_f was calculated by measuring the temperature variation of $\text{TE}_{01\delta}$ resonance mode in the temperature range 20–80 °C using Eq. 3.

$$\tau_f = (f_2 - f_1)/f_1\Delta T \quad (3)$$

where f_1 and f_2 are the resonant frequencies at 20 °C and 80 °C respectively and ΔT is the difference of initial temperature and final temperature.

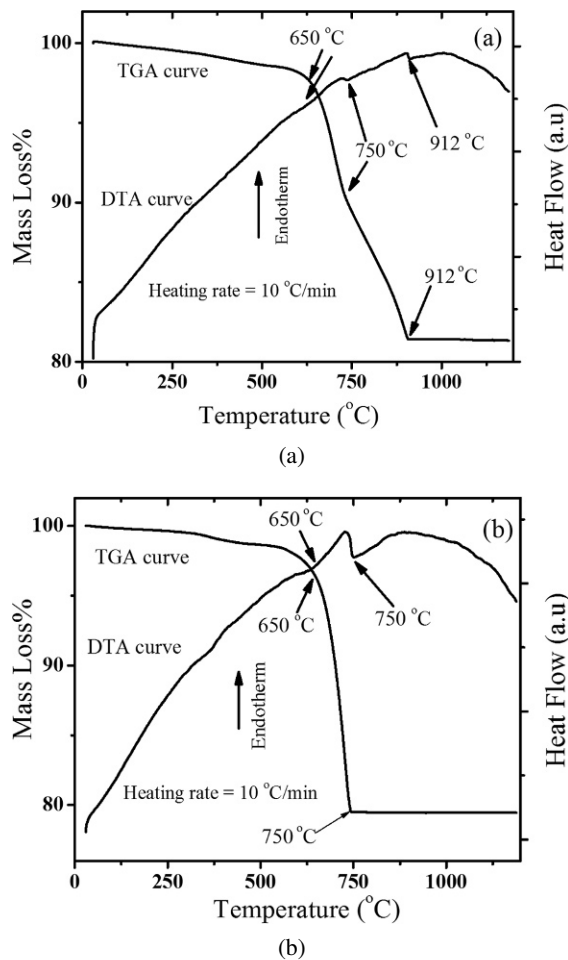


Fig. 1. TGA and DTA curves of as-mix-milled powder of a) $\text{SrCa}_4\text{Nb}_4\text{TiO}_{17}$; b) $\text{Ca}_5\text{Nb}_4\text{TiO}_{17}$ batch compositions.

3. Results and discussion

Fig. 1 shows the DTA and TGA curves for the as-mix-milled $1\text{SrCO}_3:4\text{CaCO}_3:4\text{Nb}_2\text{O}_5:1\text{TiO}_2$ (Fig. 1a) and $5\text{CaCO}_3:4\text{Nb}_2\text{O}_5:1\text{TiO}_2$ (Fig. 1b) batch composition powders. A careful examination of the TGA curve (Fig. 1a) of the $1\text{SrCO}_3:4\text{CaCO}_3:4\text{Nb}_2\text{O}_5:1\text{TiO}_2$ batch composition indicated the beginning of mass loss at 650 °C, which continued up to 750 °C, due to the decomposition of CaCO_3 [25]. Another downward slope was observed just above 750 °C which continued up to 912 °C, probably due the decomposition of SrCO_3 [12]. By flipping the DTA curve (Fig. 1a) of the as-mix-milled $1\text{SrCO}_3:4\text{CaCO}_3:4\text{Nb}_2\text{O}_5:1\text{TiO}_2$, two endotherms observed at 750 °C and 912 °C,

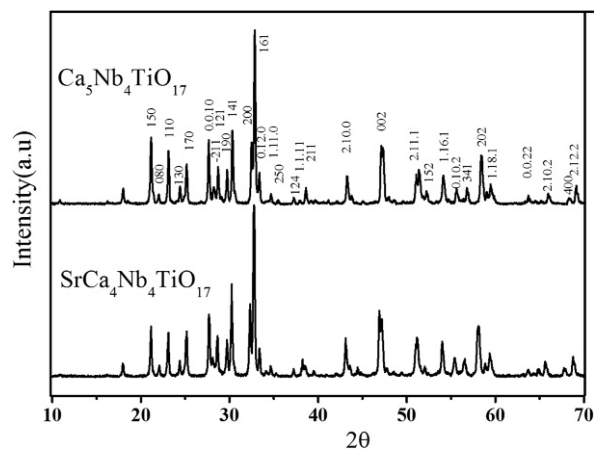


Fig. 2. XRD patterns of crushed pellets of $\text{SrCa}_4\text{Nb}_4\text{TiO}_{17}$ and $\text{Ca}_5\text{Nb}_4\text{TiO}_{17}$ sintered for 4 h, at 1450 °C and 1475 °C respectively, showing the single phase formation for each ceramics within the detection limit of employed XRD.

which is consistent with the temperature at which the downward sloping of the TGA curve ended. The observed increase in the decomposition temperature of SrCO_3 , from the previously reported 880 °C [26] to 912 °C in the present study, may be due to the increase in the heating rate from 5 °C/min to 10 °C/min [25, 26]. A total mass loss of ~ 17 % was recorded in the entire heating cycle from 30 °C to 1200 °C. Similarly, the TGA curve (Fig. 1b) of the $5\text{CaCO}_3:4\text{Nb}_2\text{O}_5:1\text{TiO}_2$ batch composition indicated the beginning of the mass loss at 650 °C, which continued up to 750 °C, due to the decomposition of CaCO_3 [14]. Only one endotherm observed in the DTA curve (Fig. 1b) at 750 °C is consistent with the temperature at which the downward sloping of TGA curve ended. A total mass loss of ~ 22 % was recorded in the entire heating cycle from 30 °C to 1200 °C. The DTA curves for both the mix milled powders did not show any exotherm above 900 °C up to 1200 °C. This indicated that the required compositions were formed at $T > 1200$ °C.

Fig. 2 shows the XRD patterns recorded for the pulverized pellets of $\text{SrCa}_4\text{Nb}_4\text{TiO}_{17}$ and $\text{Ca}_5\text{Nb}_4\text{TiO}_{17}$ ceramics sintered at 1475 °C and 1450 °C for 4 h respectively. As no PDF or JCPDS card is available for $\text{SrCa}_4\text{Nb}_4\text{TiO}_{17}$ and $\text{Ca}_5\text{Nb}_4\text{TiO}_{17}$, therefore, the patterns were indexed

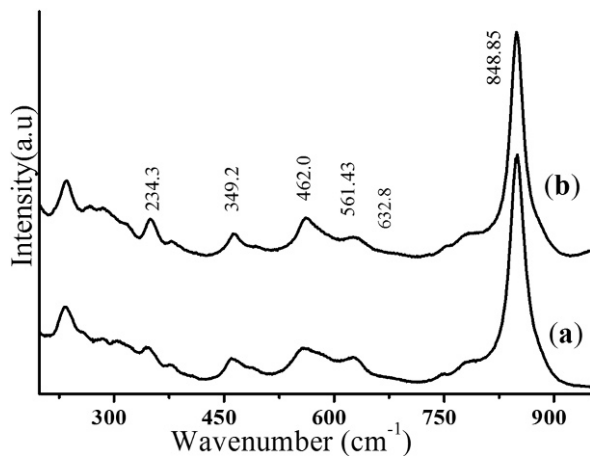


Fig. 3. Raman spectra recorded at room temperature for a) $\text{SrCa}_4\text{Nb}_4\text{TiO}_{17}$ and b) $\text{Ca}_5\text{Nb}_4\text{TiO}_{17}$.

according to the PDF# 87-1170 for $\text{Sr}_5\text{Nb}_4\text{TiO}_{17}$. The peaks positions were shifted towards smaller d -values due to the presence of Ca^{2+} with smaller ionic radii (1.34 Å) in place of Sr^{2+} (1.44 Å) for coordination number 12 [27]. No evidence of any secondary phase in both the ceramics was found. The lattice parameters of the unit cells of $\text{SrCa}_4\text{Nb}_4\text{TiO}_{17}$ and $\text{Ca}_5\text{Nb}_4\text{TiO}_{17}$, refined by the least squares method, are $a = 5.5360(5)$ Å, $b = 32.150(7)$ Å, $c = 3.870(8)$ Å, $Z = 2$, $V_m = 344.0$ Å³ for $\text{SrCa}_4\text{Nb}_4\text{TiO}_{17}$ while $a = 5.4875(7)$ Å, $b = 32.051(5)$ Å, $c = 3.8447(5)$ Å, $Z = 2$ and $V_m = 339.515$ Å³ for $\text{Ca}_5\text{Nb}_4\text{TiO}_{17}$. A previous study reported the formation of secondary phases of $(\text{Sr,Ca})_6\text{Nb}_4\text{Ti}_2\text{O}_{20}$ in $\text{SrCa}_4\text{Nb}_4\text{TiO}_{17}$ and $\text{Ca}_6\text{Nb}_4\text{Ti}_2\text{O}_{20}$ in $\text{Ca}_5\text{Nb}_4\text{TiO}_{17}$ ceramics sintered at 1500 °C for 2 h at heating/cooling rate of 10 °C/min [12].

The Raman spectra recorded at room temperature for the investigated ceramics are presented in Fig. 3. The spectra are very similar to those of the related compounds in the $\text{Ca}_{1-x}\text{Zn}_x\text{La}_4\text{Ti}_5\text{O}_{17}$ series [7]. Generally, corner sharing and edge-sharing octahedral units are predominant in (Nb,Ti)-O polyhedral. In the case of an edge-shared (Nb,Ti)O₆ octahedra the symmetric stretching vibrations are usually observed in 850–1000 cm⁻¹ region, where as in the corner-sharing octahedral units the symmetric stretching vibrations are observed in 750–850 cm⁻¹ region [28].

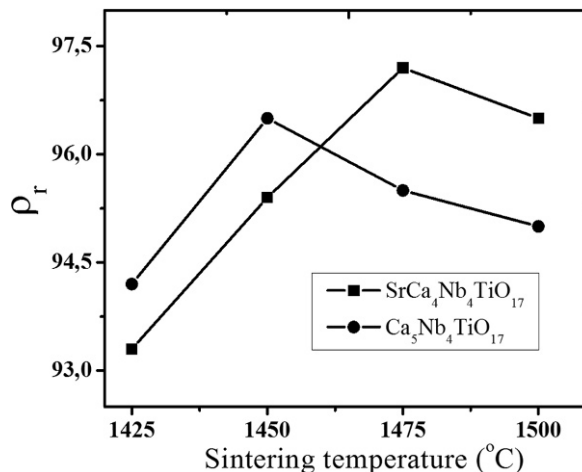
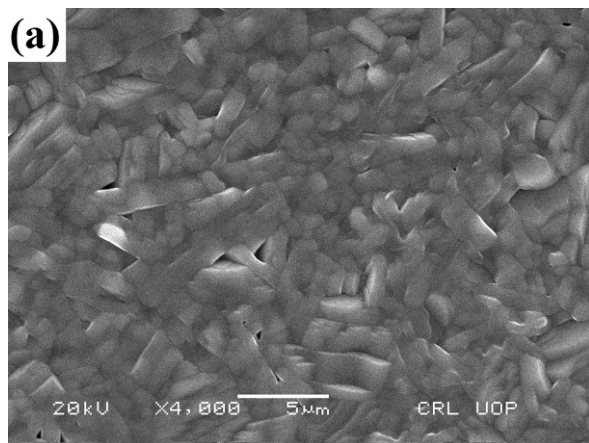


Fig. 4. Variation in the relative density (ρ_r) with sintering temperature for $\text{SrCa}_4\text{Nb}_4\text{TiO}_{17}$ and $\text{Ca}_5\text{Nb}_4\text{TiO}_{17}$, showing the optimum densities at 1475 °C and 1450 °C for $\text{SrCa}_4\text{Nb}_4\text{TiO}_{17}$ and $\text{Ca}_5\text{Nb}_4\text{TiO}_{17}$, respectively.

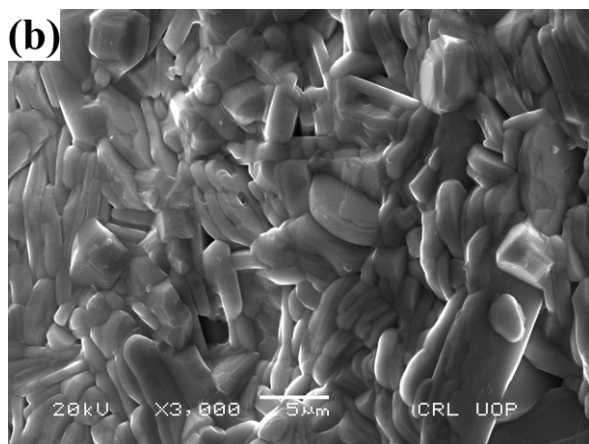
From the structural studies it is evident that the (Nb,Ti)O₆ octahedra in $\text{Ca}_5\text{Nb}_4\text{TiO}_{17}$ are corner-connected [29].

In the present study the highest frequency mode, also called A_{1g} mode at ~ 848.5 cm⁻¹ for $\text{SrCa}_4\text{Nb}_4\text{TiO}_{17}$ and $\text{Ca}_5\text{Nb}_4\text{TiO}_{17}$ corresponds to the symmetric metal-oxygen stretching vibrations of the BO₆ octahedra and supports the existence of the corner sharing octahedral units in both the compounds. The broad bands at 450 to 570 cm⁻¹ can be represented as asymmetric breathing of the BO₆ octahedra. The E_g modes in the range of 200–400 cm⁻¹ have been assigned to O–B–O bending mode [30]. The modes in the range 470–490 cm⁻¹ were described as B–O torsional modes. The modes at 314 and 464 cm⁻¹ can be attributed to the rotating and tilting of the BO₆ octahedra [30]. The weak band observed at 605–620 cm⁻¹ can be assigned to the B–O symmetric stretching vibration [30–32].

Fig. 4 shows the variation in the relative densities of $\text{SrCa}_4\text{Nb}_4\text{TiO}_{17}$ and $\text{Ca}_5\text{Nb}_4\text{TiO}_{17}$ as a function of sintering temperature. The relative density of $\text{SrCa}_4\text{Nb}_4\text{TiO}_{17}$ initially increased from ~ 93.2 % to ~ 97.5 % of its theoretical value (4.53 g/cm³) [12] as the sintering temperature was increased from 1425 °C to 1475 °C and then, with further increase in the sintering temperature to 1500 °C,



(a)



(b)

Fig. 5. SEM images of the thermally etched surface of a) $\text{SrCa}_4\text{Nb}_4\text{TiO}_{17}$ sintered at $1475\text{ }^\circ\text{C}$ and b) $\text{Ca}_5\text{Nb}_4\text{TiO}_{17}$ sintered at $1450\text{ }^\circ\text{C}$, showing plate-like shaped grains for both the compositions.

decreased to $\sim 96.5\%$ of its theoretical value, indicating that the density saturated at $1475\text{ }^\circ\text{C}$ for $\text{SrCa}_4\text{Nb}_4\text{TiO}_{17}$ ceramics. Similarly, the relative density of $\text{Ca}_5\text{Nb}_4\text{TiO}_{17}$ initially increased from $\sim 94.2\%$ to 96.5% of its theoretical value (4.41 g/cm^3) [12] as the sintering temperature was increased from $1425\text{ }^\circ\text{C}$ to $1450\text{ }^\circ\text{C}$ and then decreased to $\sim 94.9\%$ of its theoretical value with further increase in the sintering temperature to $1500\text{ }^\circ\text{C}$. This indicated that the optimum density for $\text{Ca}_5\text{Nb}_4\text{TiO}_{17}$ could be achieved at $1450\text{ }^\circ\text{C}$.

The secondary electron SEM images (SEIs) from thermally etched, gold-coated surfaces of

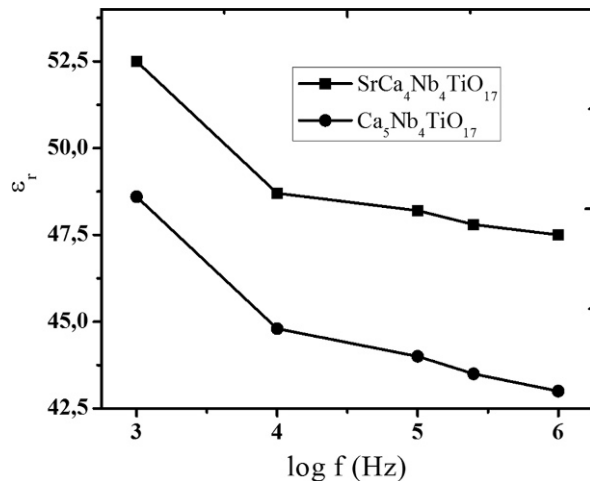


Fig. 6. Variation in ϵ_r of the optimally sintered $\text{SrCa}_4\text{Nb}_4\text{TiO}_{17}$ and $\text{Ca}_5\text{Nb}_4\text{TiO}_{17}$ ceramics as a function of frequency in the 1 kHz to 1 MHz range.

$\text{SrCa}_4\text{Nb}_4\text{TiO}_{17}$ and $\text{Ca}_5\text{Nb}_4\text{TiO}_{17}$ ceramics are shown in Fig. 5. The microstructure of both the ceramics consists of compact grains and appears to be highly dense with almost no pores, which is consistent with the observed higher relative densities (Fig. 4). The microstructure of both the ceramics is comprised of elongated and plate-like grains which is a typical morphology of the layered perovskites. The average grain size of the $\text{SrCa}_4\text{Nb}_4\text{TiO}_{17}$ ceramics does not exceed $5\text{ }\mu\text{m}$ while that of the $\text{Ca}_5\text{Nb}_4\text{TiO}_{17}$ is $\sim 8\text{ }\mu\text{m}$.

The electric permittivity (ϵ_r) of $\text{SrCa}_4\text{Nb}_4\text{TiO}_{17}$ and $\text{Ca}_5\text{Nb}_4\text{TiO}_{17}$ ceramics measured in the frequency range of 1 kHz – 1 MHz is shown in Fig. 6. The ϵ_r significantly decreased with the increase in frequency from 1 kHz to 1 MHz due to the reduction of active polarization mechanism at higher frequencies. At lower frequencies the electronic, ionic, dipolar and interfacial/surface polarizations contribute to ϵ_r , however, above 100 kHz [33], the contribution from the interfacial/surface polarization is minimized and results in a decrease in ϵ_r from 52 to 47.5 and from 48.7 to 43.2 for $\text{SrCa}_4\text{Nb}_4\text{TiO}_{17}$ and $\text{Ca}_5\text{Nb}_4\text{TiO}_{17}$ ceramics, respectively.

Both the ceramics showed good resonance at microwave frequencies. The microwave dielectric properties of $\text{SrCa}_4\text{Nb}_4\text{TiO}_{17}$ and $\text{Ca}_5\text{Nb}_4\text{TiO}_{17}$

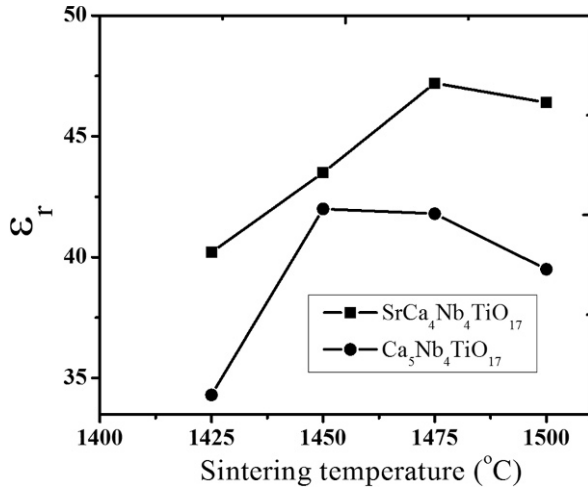


Fig. 7. Variation in ϵ_r of $\text{SrCa}_4\text{Nb}_4\text{TiO}_{17}$ and $\text{Ca}_5\text{Nb}_4\text{TiO}_{17}$ as a function of sintering temperature, showing optimum ϵ_r at 1475 °C.

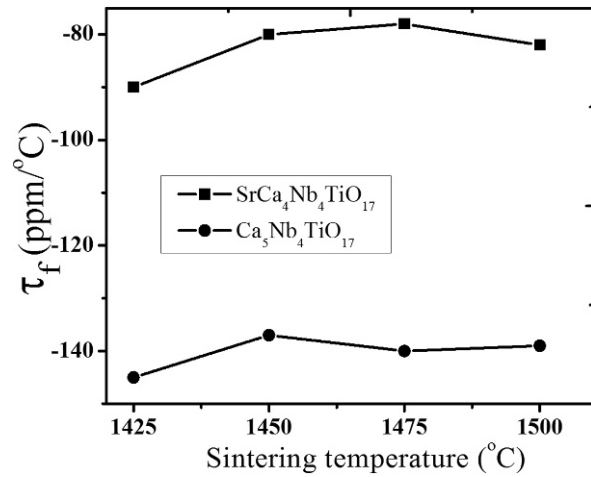


Fig. 9. Variation in τ_f of $\text{SrCa}_4\text{Nb}_4\text{TiO}_{17}$ and $\text{Ca}_5\text{Nb}_4\text{TiO}_{17}$ ceramics as a function of sintering temperature.

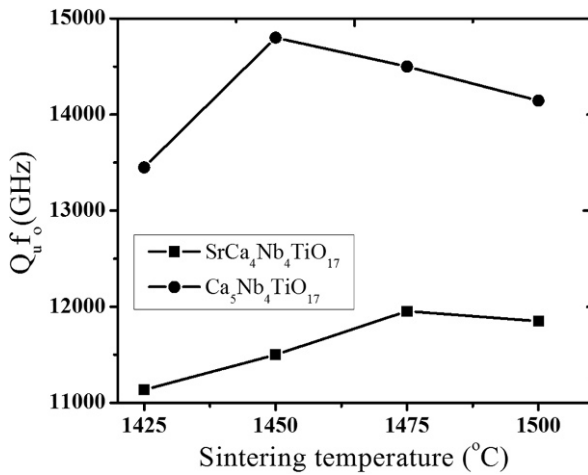


Fig. 8. Variation in Q_{uf_o} of $\text{SrCa}_4\text{Nb}_4\text{TiO}_{17}$ and $\text{Ca}_5\text{Nb}_4\text{TiO}_{17}$ as a function of sintering temperature.

sintered in the temperature range of 1425 °C to 1500 °C are shown in Figs. 7–9. All the three properties *i.e.* ϵ_r , τ_f and Q_{uf_o} show the same trend with the sintering temperature as the relative density. $\text{SrCa}_4\text{Nb}_4\text{TiO}_{17}$, sintered at optimum sintering temperature of 1475 °C for 4 h exhibited $\epsilon_r \sim 47.2$, $Q_{uf_o} \sim 11954$ GHz and $\tau_f \sim -78$ ppm/K. Similarly, $\text{Ca}_5\text{Nb}_4\text{TiO}_{17}$, sintered at optimum sintering temperature of 1450 °C for 4 h exhibited, $\epsilon_r \sim 42$, $Q_{uf_o} \sim 14800$ GHz and $\tau_f \sim -137$ ppm/K. The decrease in ϵ_r for $\text{Ca}_5\text{Nb}_4\text{TiO}_{17}$ in comparison to

$\text{SrCa}_4\text{Nb}_4\text{TiO}_{17}$ is due to the presence of Ca^{2+} characterized by lower ionic dielectric polarizability (3.16 \AA^3) in comparison to Sr^{2+} (4.24 \AA^3) [34]. It was also reported that large volume of cation site at the A site of the layered perovskite results in a large ϵ_r . The volume of the cation site in the $\text{SrCa}_4\text{Nb}_4\text{TiO}_{17}$ unit cell is larger in comparison to $\text{Ca}_5\text{Nb}_4\text{TiO}_{17}$ unit cell due to the presence of Sr with larger ionic radius (1.44 \AA) as compared to Ca (1.34 \AA) for coordination number 12 [27] which resulted in the increase of ϵ_r for $\text{SrCa}_4\text{Nb}_4\text{TiO}_{17}$ ceramics. Reaney and Idles [4] suggested that ϵ_r is directly proportional to τ_f in the absence of any structural phase transition within the solid solution. Therefore, the incorporation of Ca^{2+} instead of Sr^{2+} led to a tilting of the BO_6 octahedra which caused a decrease in the τ_f from -78 ppm/K to -137 ppm/K. In a previous study the authors have reported $Q_{uf_o} \sim 1664$ GHz and $Q_{uf_o} \sim 3087$ GHz for $\text{SrCa}_4\text{Nb}_4\text{TiO}_{17}$ and $\text{Ca}_5\text{Nb}_4\text{TiO}_{17}$ sintered at 1500 °C for 2 h at heating/cooling rate of $10 \text{ }^\circ\text{C}/\text{min}$ [12] which was much lower than that in the present study. The achievement of better Q_{uf_o} values for both the ceramics may be due to the absence of any secondary phase(s) as it was observed in the previous study. This also may result from employing the different processing conditions. In another study [13], which employed the same processing condi-

tions as in the present study, $Q_{uf_o} \sim 17000$ GHz was reported for $\text{Ca}_5\text{Nb}_4\text{TiO}_{17}$. Thus the appropriate processing conditions led to a single phase formation during the calcination and sintering processes which resulted in an improvement in the microwave dielectric properties of both $\text{SrCa}_4\text{Nb}_4\text{TiO}_{17}$ and $\text{Ca}_5\text{Nb}_4\text{TiO}_{17}$ ceramics.

4. Conclusions

$\text{SrCa}_4\text{Nb}_4\text{TiO}_{17}$ and $\text{Ca}_5\text{Nb}_4\text{TiO}_{17}$, sintered at 1475 °C and 1450 °C for 4 h, crystallized in a single phase ceramics with the microstructure comprised of elongated and plate-like grains. In the most favorable sintering conditions, the optimum microwave dielectric properties *i.e.* $\tau_f \sim -78$ ppm/K, $\epsilon_r \sim 47.2$ and $Q_{uf_o} \sim 11954$ for $\text{SrCa}_4\text{Nb}_4\text{TiO}_{17}$, and $\tau_f \sim -137$ ppm/K, $\epsilon_r \sim 42$ and $Q_{uf_o} \sim 14800$ GHz for $\text{Ca}_5\text{Nb}_4\text{TiO}_{17}$ were achieved. The different processing conditions employed in the present study resulted in the improvement of the microwave properties of the ceramics with the same compositions as in the previous study. Further study is in progress to tune the τ_f of the ceramics to zero for possible microwave applications.

Acknowledgements

The authors acknowledge the financial support of the Higher Education Commission of Pakistan and electroceramics group at the department of Materials Science and Engineering University of Sheffield UK.

References

- [1] NEDELCO L., TOACSAN M.I., BANCUI M.G., LOACHIM A., *J. Alloys. Compd.*, 509 (2011), 477.
- [2] OHSATO H., *J. Ceram. Soc. Jap.*, 113 (11) (2005), 703.
- [3] FREER R., AZOUGH F., *J. Euro. Ceram. Soc.*, 28 (2008), 1433.
- [4] REANEY I.M., IDLES D., *J. Am. Ceram. Soc.*, 89 (7) (2006), 2068.
- [5] SEBASTIAN M.T., *Dielectric Materials for Wireless Communication*, Elsevier LTD, 2008.
- [6] JAWAHAR I.N. SANTHA N. SEBASTIAN M.T., MOHANAN P., *J. Mater. Res.*, 17 (2002), 3084.
- [7] FEI Z. ZHENXING Y. ZHILUN G., LONGTU L., *J. Am. Ceram. Soc.*, 89 (11) (2006), 3421.
- [8] CHEN Y.C., TSAI J.M., *JPN. J. APPL. PHYS.*, 47 (2008), 7959.
- [9] CHEN Y.C., YAO S.L., CHEN R.J., K.C., *J. Alloys. Compd.*, 486 (2009), 410.
- [10] IQBAL Y., MANAN A., REANEY I.M., *Mater. Res. Bull.*, 46(7) (2011), 1092.
- [11] MANAN A., IQBAL Y., *J. Mater. Sci. Mater. Electron.*, 22(12) (2011), 1848.
- [12] MANAN A., IQBAL Y., QAZI I., *J. Mater. Sci.*, 46(10) (2011), 3415.
- [13] JOSEPH T., ANJANA P.S., LETOURNEAU S., UBIC R., SMAALEN S.V., SEBASTIAN M.T., *Mater. Chem. Phys.*, 121 (2010) 77.
- [14] CHEN G.H., DI J.C., XU H.R., YANG Y., YUAN C.L., ZHOU C.R., CHENG J., KIU X.Y., *J. Mater. Sci. Mater. Electron.*, 23(1) (2012), 280.
- [15] ICHINOSE N.T., SHIMADA, *J. Euro. Ceram. Soc.*, 26 (2006), 1755.
- [16] MCNEAL M.P., JANG S.J.R., NEWNHAM E., *J. Appl. Phys.*, 83(6) (1998), 3288.
- [17] ROULLAND F. TERRAS R., MARINEL S., *Mater. Sci. Eng. B.*, 104 (2003), 156.
- [18] TSENG C.F., HUANG C.L., YANG W.R., HSU. C.H., *J. Am. Ceram. Soc.*, 89 (4) (2006), 1465.
- [19] KAN A., OGAWA H., OHSATO H., *J. Alloys. Compd.*, 337 (2002), 303.
- [20] FANG Y., HU A., OUYANG S., OH J.J., *J. Euro. Ceram. Soc.*, 21(2001), 2745.
- [21] OISHI T., OGAWA H., KAN A., *Mater. Res. Bull.*, 42 (2007), 2072.
- [22] NEGAS T., YEAGER G., BELL S., COATES N., MINIS I., *Am. Ceram. Soc. Bull.*, 72 (1993), 80.
- [23] DESHPANDE V.V., PATIL M.M., RAVI V., *Ceram. Inter.*, 32(3) (2006), 353.
- [24] KRUPKA J., DERZAKOWSKI K., RIDDLE B., BAKER-JARVIS J., *Meas. Sci. Technol.*, 9 (1998), 1751.
- [25] SINTON C.W., *Raw materials for glass and ceramics sources, processes and quality control*, John Willey & Son Inc, 2006, p. 151–160.
- [26] MANAN A., IQBAL Y., QAZI I., *J. Pak. Mater. Soc.*, 2(2) (2008), 77.
- [27] SHANNON R.D., *Acta. Cryst. A.*, 32 (1976) 751.
- [28] RATHEESH R., SREEMOOLANADHAN H., SEBASTIAN M.T., *J. Solid. State. Chem.*, 131 (1997), 2.
- [29] TITOV Y.A., BELYAVINA N.M., MARKIVE V.Y., SLOBODYANIK M.S., CHUMAK V.V., *J. Alloys. Compd.*, 387 (2005) 82.
- [30] HAO H., LIU H.X., CAO M.H., MIN X.M., OUYANG S.X., *Appl. Phys. A.*, 85 (2006), 69.
- [31] ZHENG H. ET AL., *J. Mater. Res.*, 19 (2004) 488.
- [32] HIRATA T., ISHIOKA K.M., KITAJIMA, *J. Solid. State. Chem.*, 124 (1996), 353.
- [33] FANG L., DIAO C.L., ZHANG H., YOAN R.Z., DRONSKOWSKI R., LIU H.X., *J. Mater. Sci. Mater. Electron.*, 15 (2004), 803.
- [34] SHANNON R.D., *J. Appl. Phys.*, 73 (1993), 348.

Received 27.01.2012
Accepted 25.05.2012